

Supporting Information

**3c/4e $\hat{\sigma}$ -Type Long-Bonding Competes with ω -Bonding in
Noble-Gas Hydrides HNgY ($\text{Ng} = \text{He, Ne, Ar, Kr, Xe, Rn}$; $\text{Y} = \text{F, Cl, Br, I}$): NBO/NRT Perspective**

Table S1. The NRT weightings of three resonance structures (ω_i , ω_{ii} , ω_{iii} for RSI, RSII, RSIII , respectively, %) and the second-order perturbation stabilization energies ($\Delta E^{(2)}_{D \rightarrow A}$ kcal/mol) for HArF with different basis sets.

basis set	ω_i	ω_{ii}	ω_{iii}	$\Delta E^{(2)}_{nY \rightarrow o^*HN_g}$	$\Delta E^{(2)}_{nH \rightarrow o^*NgY}$	$\Delta E^{(2)}_{nNg \rightarrow o^*HY}$
6-311++G**	65.06	5.64	29.29	41.46	676.97	362.83
aug-cc-pVDZ	66.37	4.87	28.76	35.11	564.24	354.09
aug-cc-pVTZ	67.10	5.18	27.72	39.76	679.97	362.97
aug-cc-pVQZ	67.48	6.45	26.07	37.71	695.79	370.84

Table S2. NPA charge (Q) of the HN_gY species calculated at B3LYP/aug-cc-pVTZ(-pp) level of theory

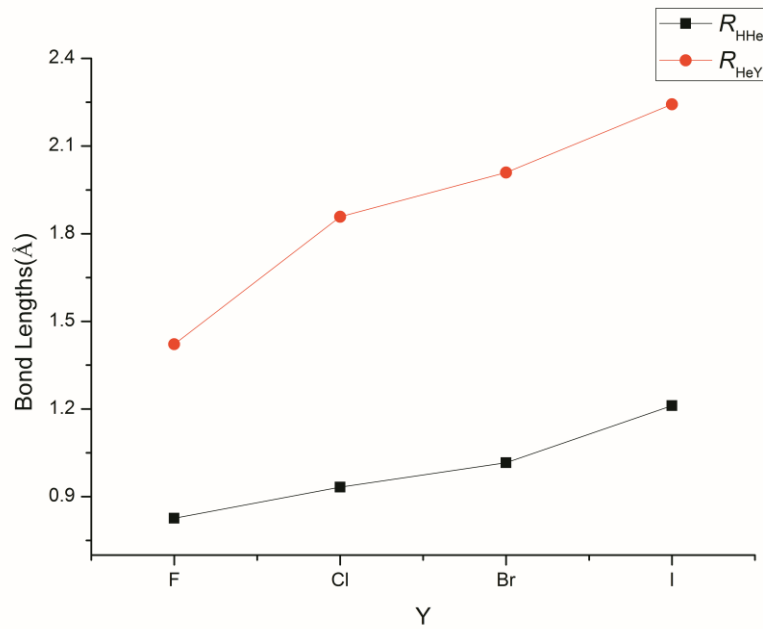
Species	Q(H)	Q(N_g)	Q(Y)
HHeF	0.322	0.328	-0.651
HHeCl	0.261	0.231	-0.492
HHeBr	0.207	0.190	-0.397
HHel	0.109	0.127	-0.235
HNeF	0.403	0.178	-0.581
HNrCl	0.242	0.098	-0.340
HNeBr	0.171	0.072	-0.243
HNel	0.080	0.047	-0.126
HArF	0.202	0.510	-0.712
HArCl	0.185	0.413	-0.598
HArBr	0.162	0.375	-0.537
HArI	0.112	0.317	-0.429
HKrF	0.090	0.632	-0.723
HKrCl	0.090	0.523	-0.613
HKrBr	0.076	0.484	-0.5603
HKrI	0.047	0.429	-0.4763
HXeF	-0.034	0.781	-0.746
HXeCl	-0.023	0.658	-0.635
HXeBr	-0.029	0.617	-0.587
HXeI	-0.045	0.563	-0.518
HRnF	-0.081	0.843	-0.762
HRnCl	-0.068	0.720	-0.652
HRnBr	-0.073	0.678	-0.605
HRnI	-0.088	0.624	-0.536

Table S3. Covalent, electrovalent (Ionic), and total contributions to the bond orders (b_{HNg} , b_{NgY} , b_{HY}) of the HNgY species at the B3LYP/aug-cc-pVTZ(-pp) level of theory.

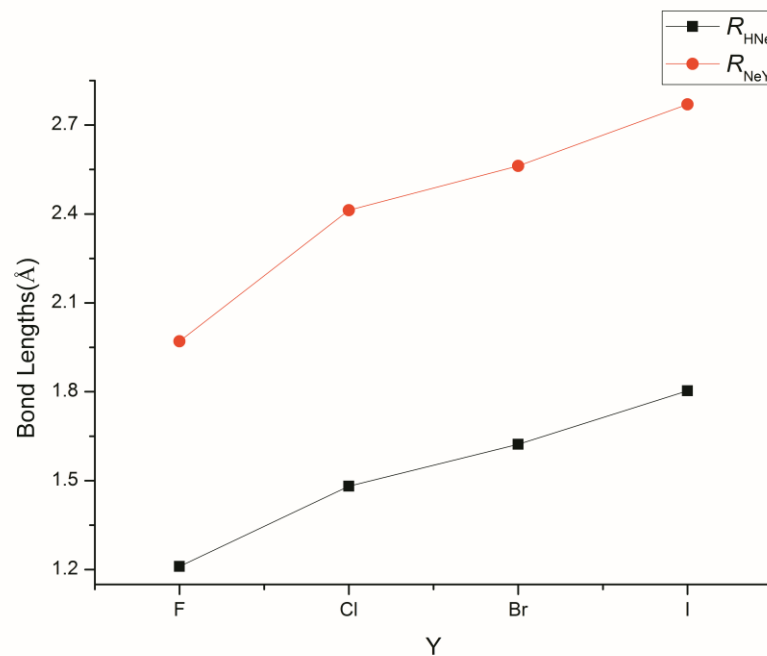
Species	b_{HNg}			b_{NgY}			b_{HY}			Sum
	Total	Covalent	Ionic	Total	Covalent	Ionic	Total	Covalent	Ionic	
HHeF	0.48	0.16	0.32	0.04	0.04	0.00	0.48	0.16	0.32	1.00
HHeCl	0.28	0.07	0.21	0.04	0.03	0.01	0.68	0.32	0.36	1.00
HHeBr	0.21	0.05	0.16	0.05	0.02	0.03	0.74	0.41	0.32	1.00
HHeI	0.12	0.02	0.10	0.06	0.01	0.05	0.82	0.59	0.23	1.00
HNeF	0.27	0.05	0.22	0.03	0.01	0.2	0.70	0.28	0.42	1.00
HNeCl	0.12	0.02	0.10	0.03	0.01	0.02	0.85	0.54	0.31	1.00
HNeBr	0.07	0.01	0.06	0.04	0.01	0.03	0.89	0.66	0.23	1.00
HNeI	0.04	0.00	0.04	0.03	0.0-	0.03	0.93	0.80	0.13	1.00
HArF	0.67	0.34	0.33	0.05	0.03	0.02	0.28	0.08	0.20	1.00
HArCl	0.56	0.23	0.33	0.06	0.05	0.01	0.38	0.15	0.23	1.00
HArBr	0.45	0.18	0.29	0.06	0.06	0.00	0.49	0.21	0.28	1.00
HArI	0.36	0.13	0.23	0.07	0.05	0.02	0.56	0.30	0.26	1.00
HKrF	0.71	0.44	0.27	0.08	0.04	0.04	0.21	0.06	0.15	1.00
HKrCl	0.60	0.31	0.29	0.08	0.06	0.02	0.32	0.13	0.19	1.00
HKrBr	0.51	0.26	0.25	0.08	0.07	0.01	0.41	0.17	0.24	1.00
HKrI	0.44	0.20	0.24	0.09	0.09	0.00	0.47	0.23	0.24	1.00
HXeF	0.74	0.56	0.18	0.11	0.04	0.07	0.15	0.04	0.11	1.00
HXeCl	0.65	0.41	0.24	0.09	0.06	0.03	0.26	0.10	0.16	1.00
HXeBr	0.58	0.36	0.22	0.16	0.08	0.08	0.26	0.12	0.14	1.00
HXeI	0.50	0.29	0.21	0.14	0.10	0.04	0.36	0.17	0.19	1.00
HRnF	0.75	0.60	0.15	0.12	0.04	0.08	0.13	0.04	0.09	1.00
HRnCl	0.65	0.44	0.21	0.14	0.07	0.07	0.21	0.08	0.13	1.00
HRnBr	0.57	0.38	0.19	0.15	0.08	0.07	0.28	0.11	0.17	1.00
HRnI	0.52	0.32	0.20	0.16	0.10	0.06	0.32	0.15	0.17	1.00

Figure S1. Trends in bond lengths (R_{HgY} and R_{NgY} , Å) in the HHeY (a), HNeY (b), HArY (c), HKrY (d), HRnY (e), Y= F, Cl, Br, I species.

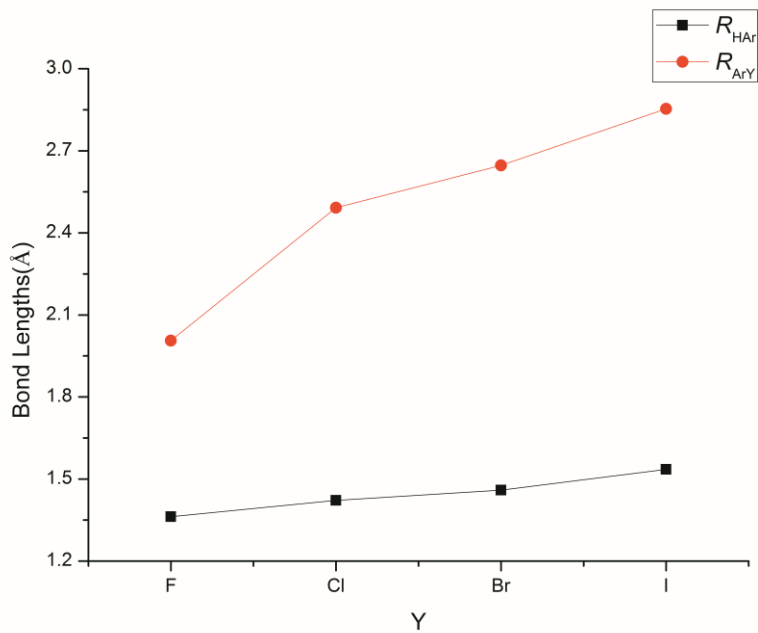
(a)HHeY



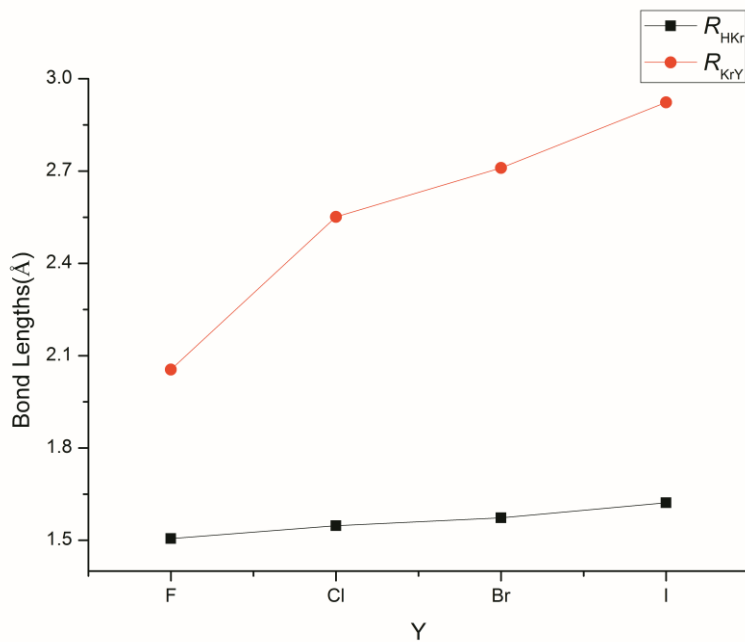
(b)HNeY



(c)HArY



(d)HKrY



(e)HRnY

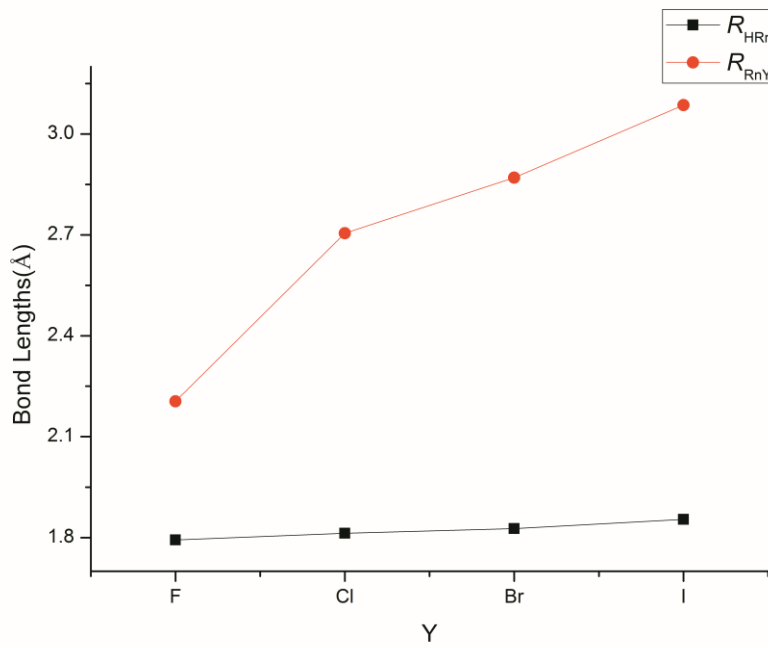


Figure S2. 3-D surface views of the $n_{He} \rightarrow \delta_{HI}$ donor-acceptor interaction in HHeI.

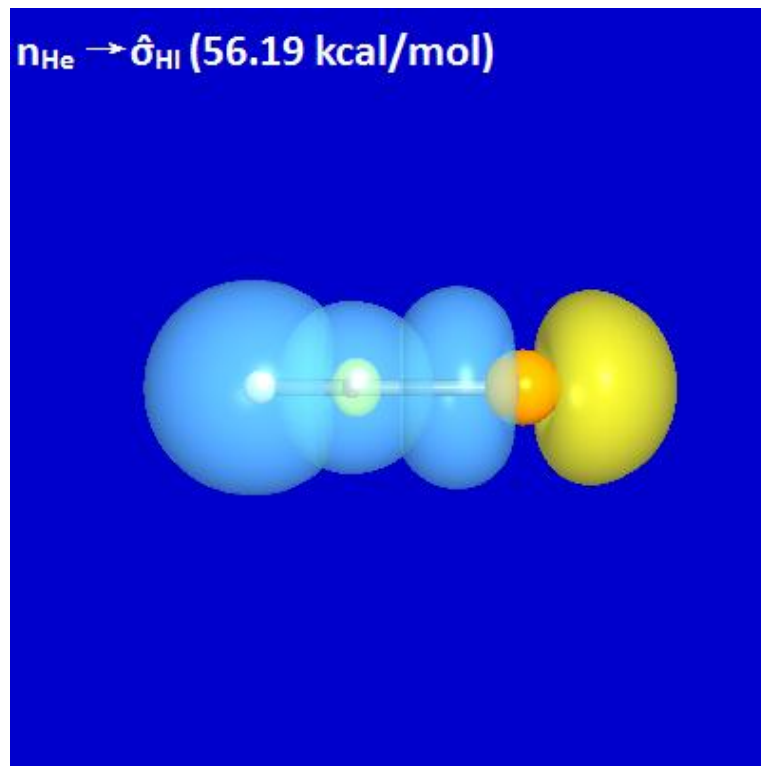
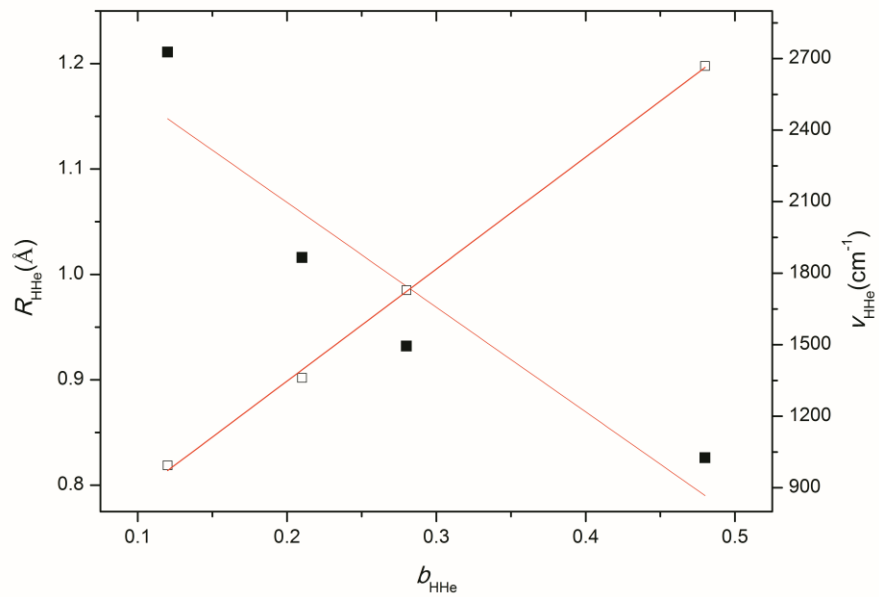


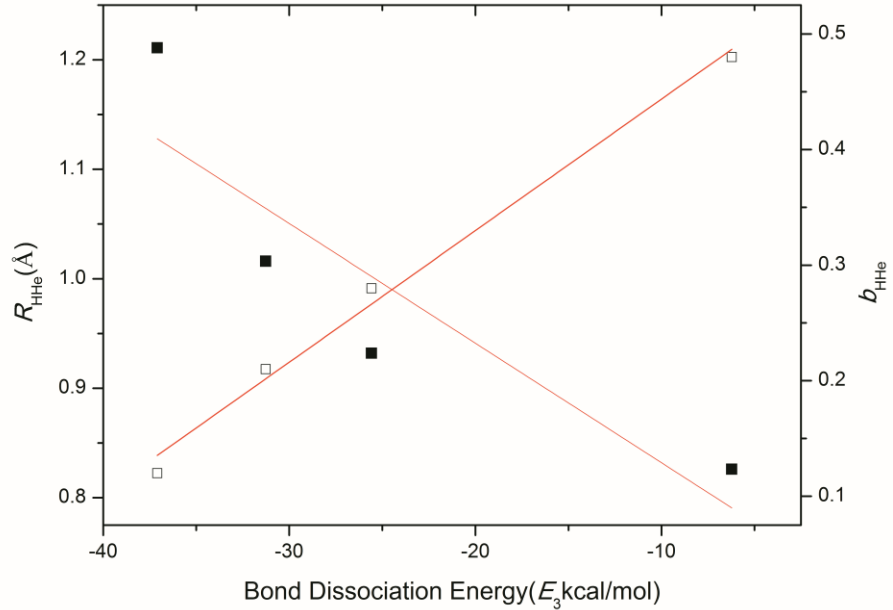
Figure S3. The results of linear correlation for HNgY (Ng= He, Ne, Kr, Xe, Rn; Y= F, Cl, Br I)

HHeY (Y= F, Cl, Br, I)

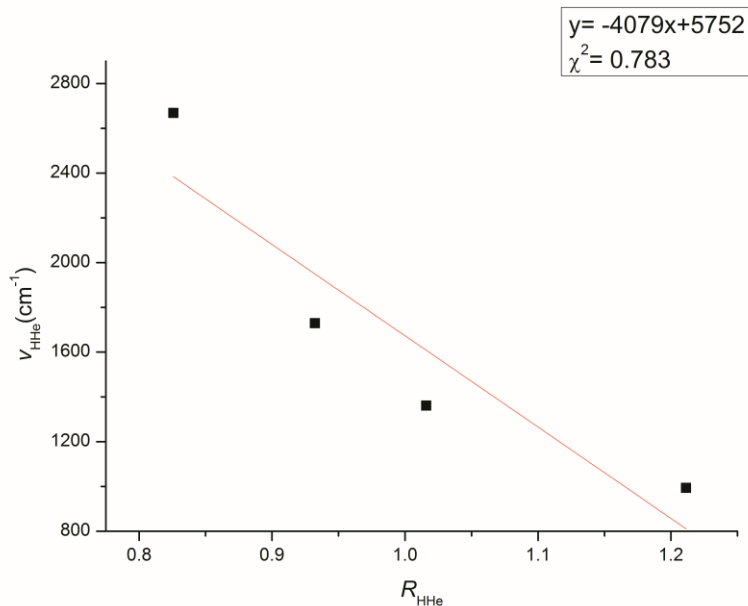
(a) Correlation plots for bond order-bond length ($\chi^2=0.806$ for $b_{\text{HHe}}-R_{\text{HHe}}$) and bond order-bond frequency ($\chi^2=0.998$ for $b_{\text{HHe}}-\nu_{\text{HHe}}$) in HHeY.



(b) Correlation plots for bond dissociation energy-bond length ($\chi^2=0.710$ for E_3-R_{HHe}) and bond dissociation energy-bond order ($\chi^2=0.989$ for E_3-b_{HHe}) in HHeY.

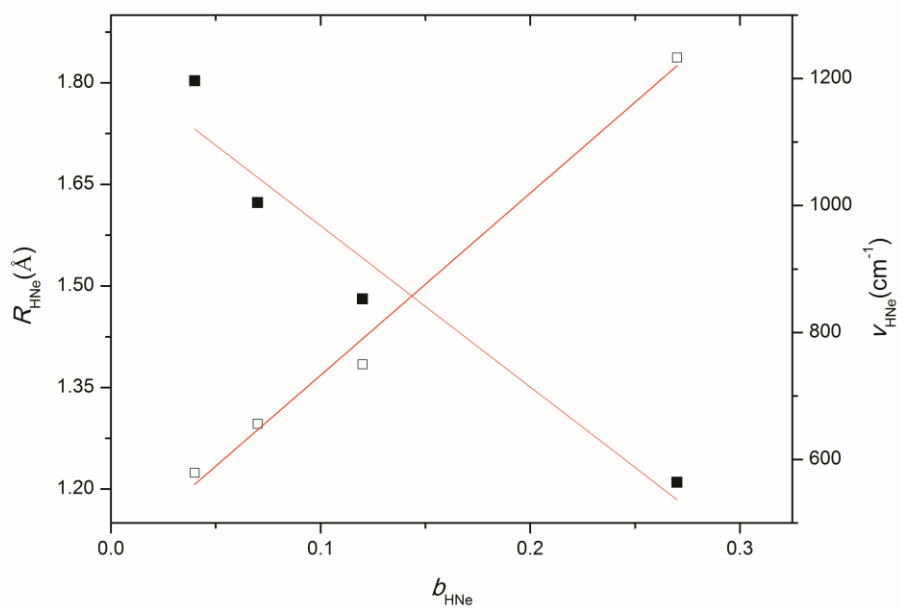


(c) Correlation plots for bond length-bond frequency ($\chi^2=0.783$ for $R_{\text{HHe}}-V_{\text{HHe}}$) in HHeY.

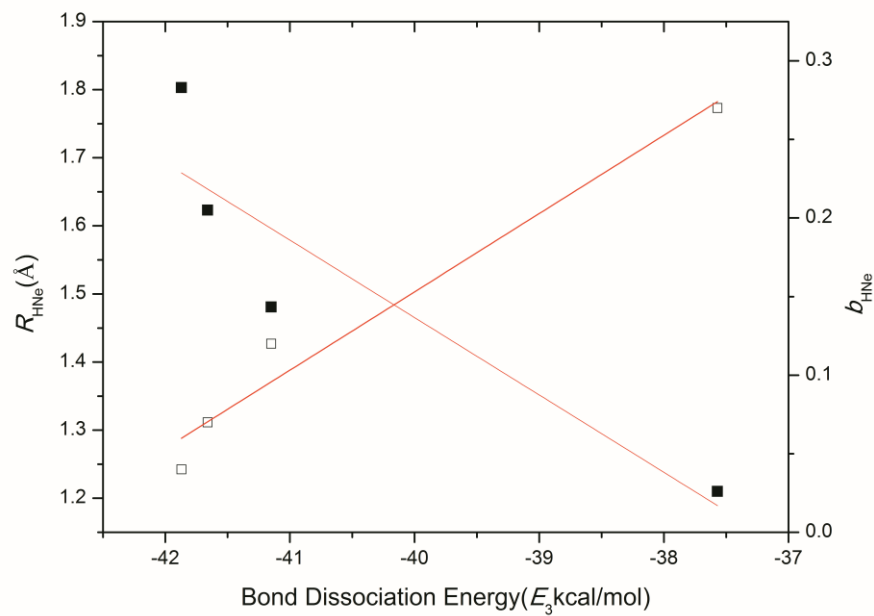


HNeY (Y= F, Cl, Br, I)

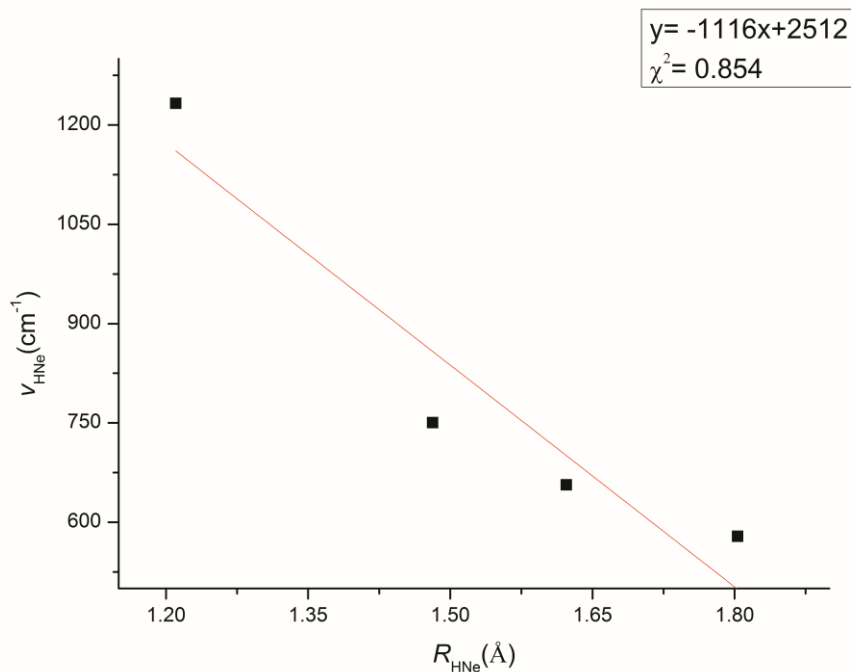
(a)Correlation plots for bond order-bond length ($\chi^2=0.914$ for $b_{\text{HNe}}-R_{\text{HNe}}$) and bond order-bond frequency ($\chi^2=0.987$ for $b_{\text{HNe}}-V_{\text{HNe}}$) in HNeY.



(b) Correlation plots for bond dissociation energy-bond length ($\chi^2=0.758$ for E_3-R_{HNe}) and bond dissociation energy-bond order ($\chi^2=0.952$ for E_3-b_{HNe}) in HNeY.

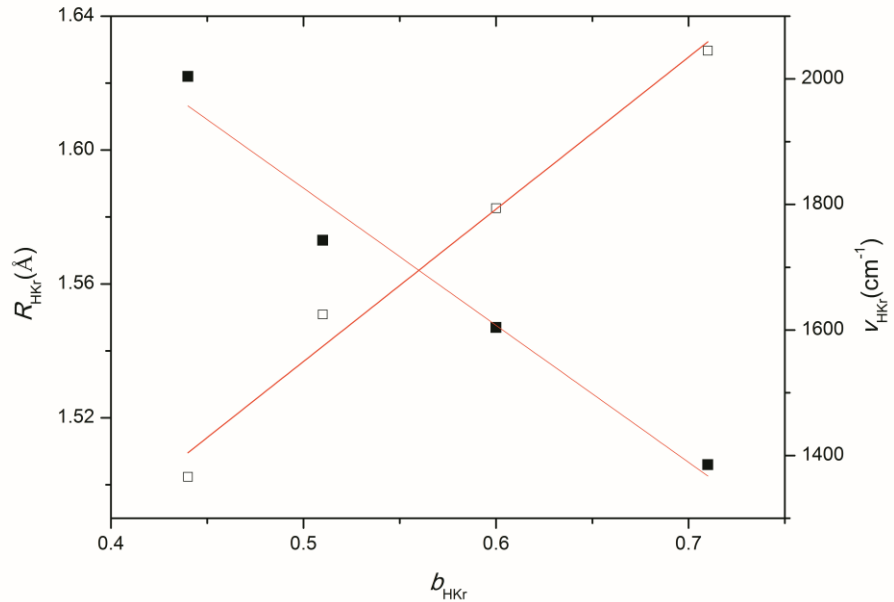


(c) Correlation plots for bond length-bond frequency ($\chi^2=0.854$ for $R_{\text{HNe}}-V_{\text{HNe}}$) in HNeY.

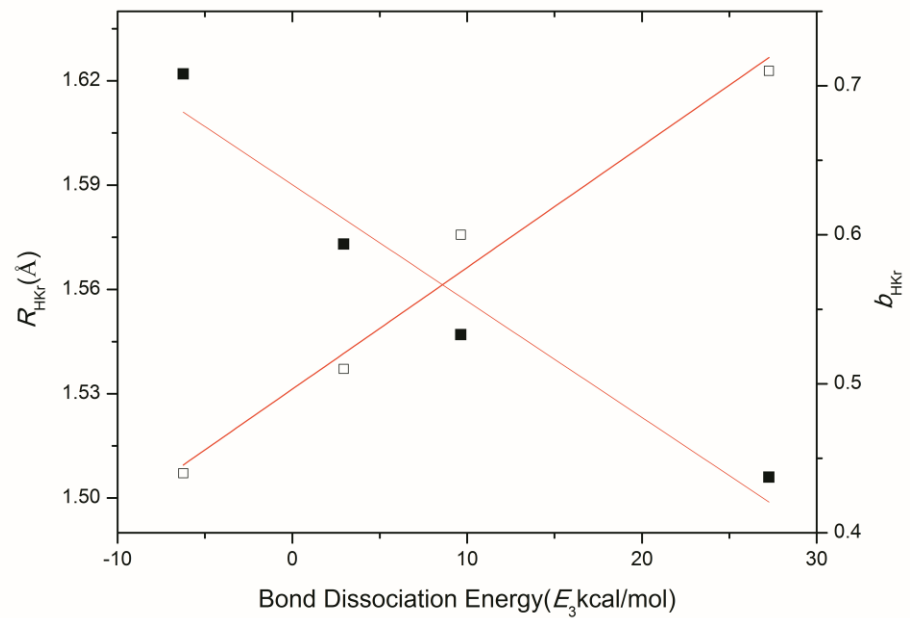


HKrY (Y= F, Cl, Br, I)

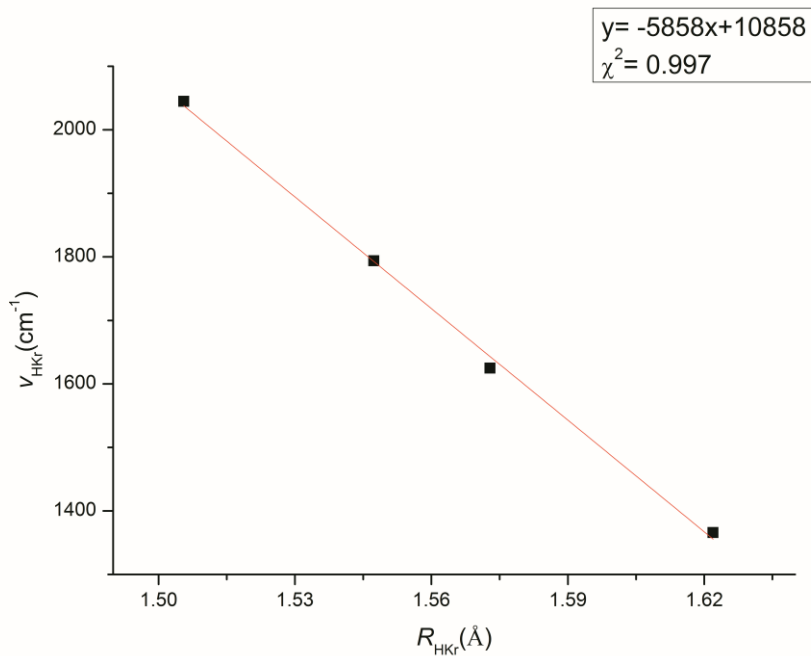
(a) Correlation plots for bond order-bond length ($\chi^2=0.953$ for $b_{\text{HKr}}-R_{\text{HKr}}$) and bond order-bond frequency ($\chi^2=0.974$ for $b_{\text{HKr}}-v_{\text{HKr}}$) in HKrY.



(b) Correlation plots for bond dissociation energy-bond length ($\chi^2=0.927$ for E_3-R_{HKr}) and bond dissociation energy-bond order ($\chi^2=0.969$ for E_3-b_{HKr}) in HKrY.

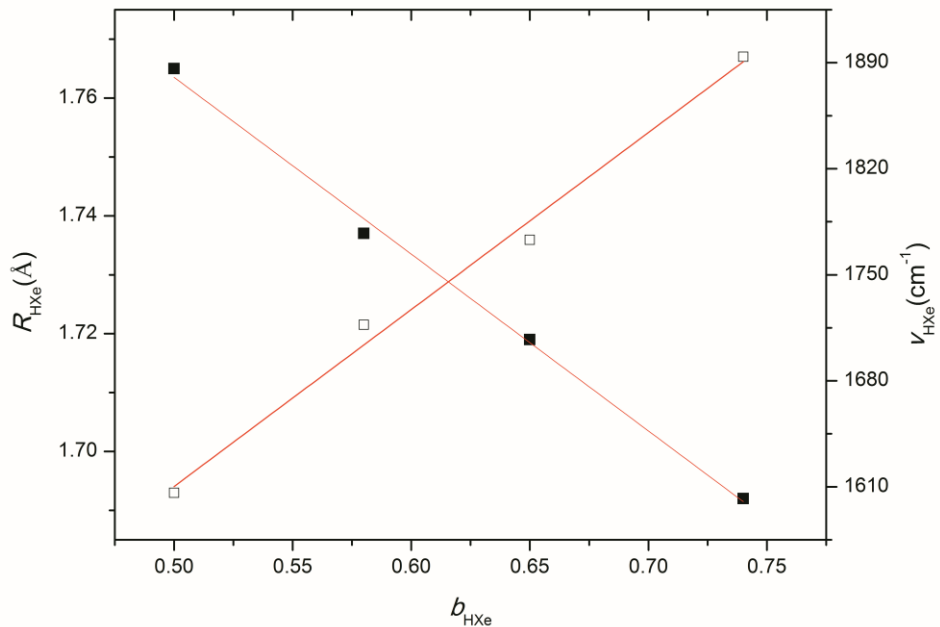


(c) Correlation plots for bond length-bond frequency ($\chi^2=0.997$ for $R_{\text{HKr}}-v_{\text{HKr}}$) in HKrY.

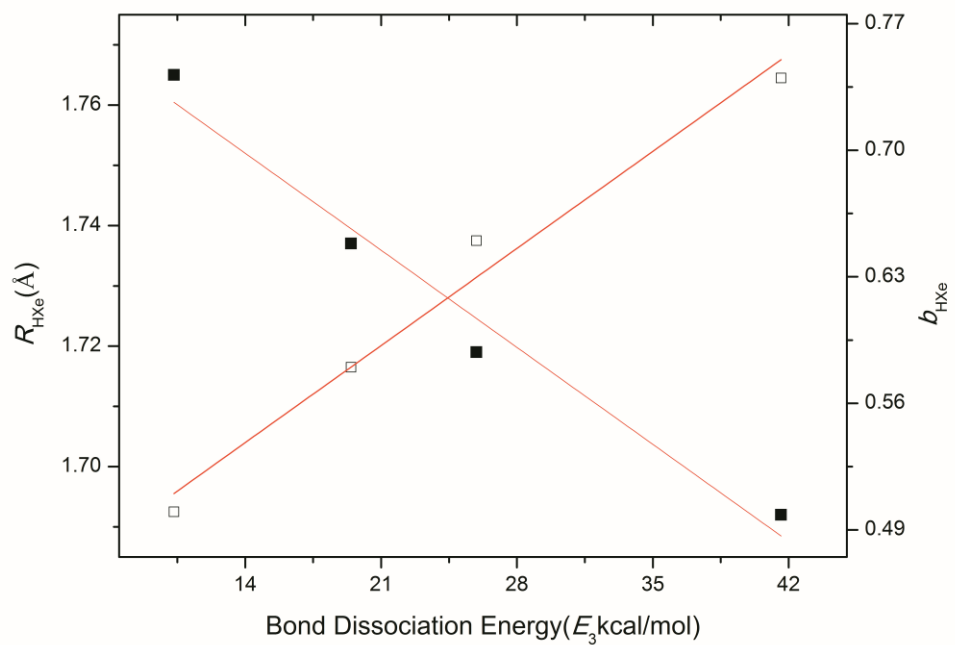


HXeY (Y=F, Cl, Br, I)

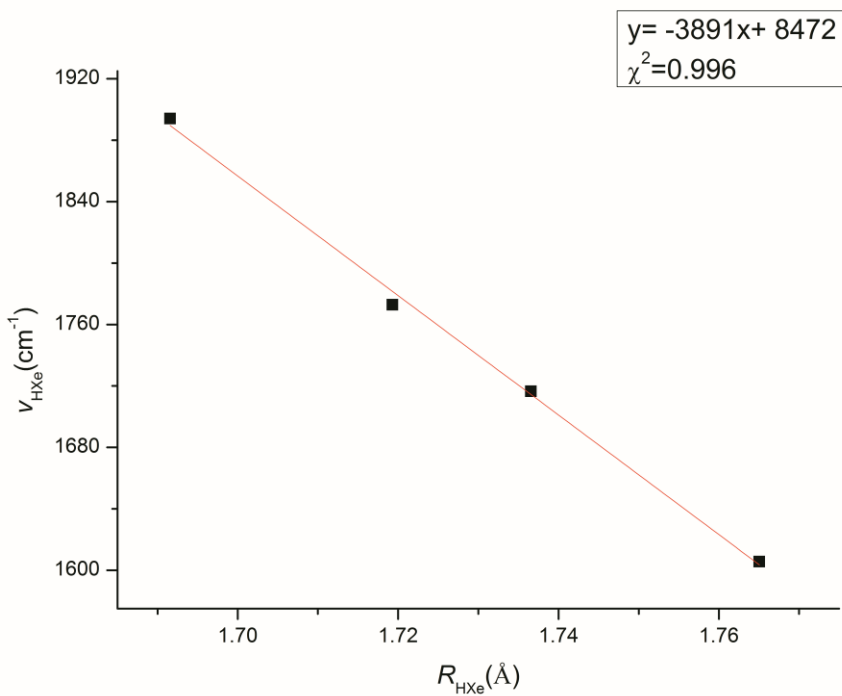
(a)Correlation plots for bond order-bond length ($\chi^2=0.995$ for $b_{\text{HXe}}-R_{\text{HXe}}$) and bond order-bond frequency ($\chi^2=0.987$ for $b_{\text{HXe}}-v_{\text{HXe}}$) in HXeY.



(b) Correlation plots for bond dissociation energy-bond length ($\chi^2=0.962$ for E_3-R_{HXe}) and bond dissociation energy-bond order ($\chi^2=0.970$ for E_3-b_{HXe}) in HXeY.

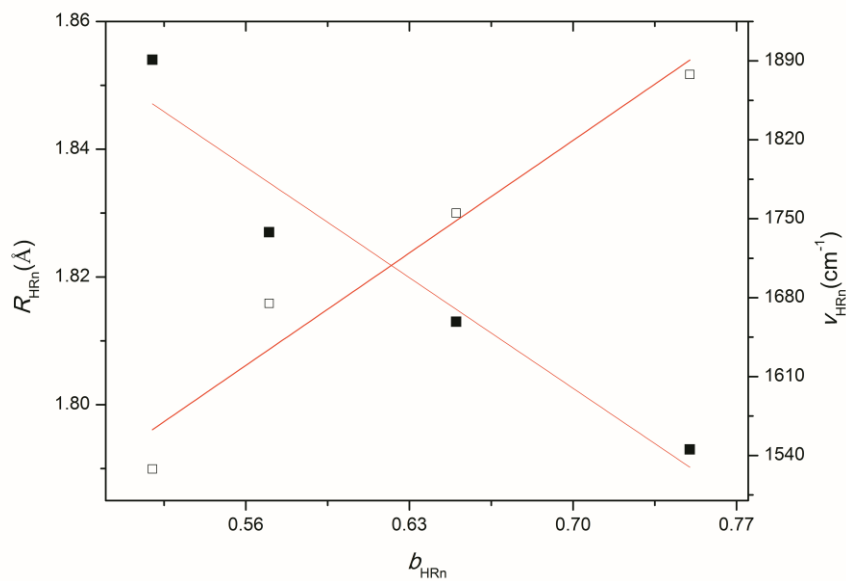


(c) Correlation plots for bond length-bond frequency ($\chi^2=0.996$ for $R_{\text{HXe}}-v_{\text{HXe}}$) in HXeY.

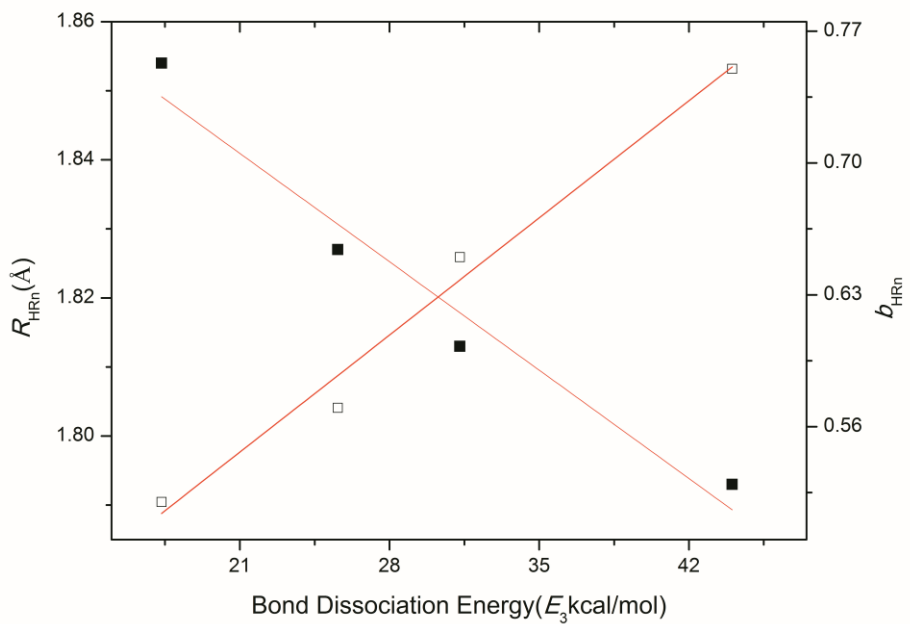


HRnY (Y= F, Cl, Br, I)

(a) Correlation plots for bond order-bond length ($\chi^2=0.909$ for $b_{\text{HRn}}-R_{\text{HRn}}$) and bond order-bond frequency ($\chi^2=0.928$ for $b_{\text{HRn}}-v_{\text{HRn}}$) in HRnY.



(b) Correlation plots for bond dissociation energy-bond length ($\chi^2=0.944$ for E_3-R_{HRn}) and bond dissociation energy-bond order ($\chi^2=0.976$ for E_3-b_{HRn}) in HRnY.



(c) Correlation plots for bond length-bond frequency ($\chi^2=0.998$ for $R_{\text{HRn}}-v_{\text{HRn}}$) in HRnY.

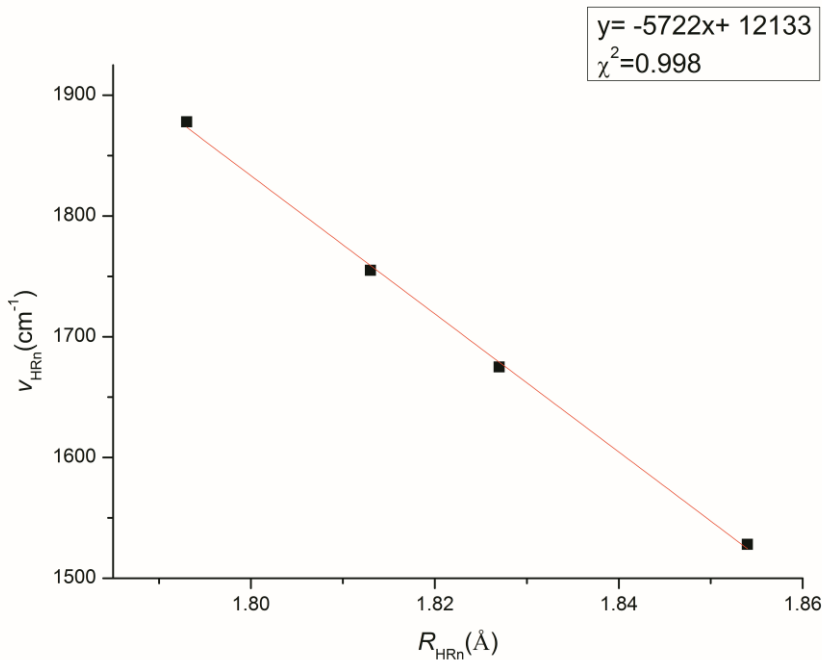
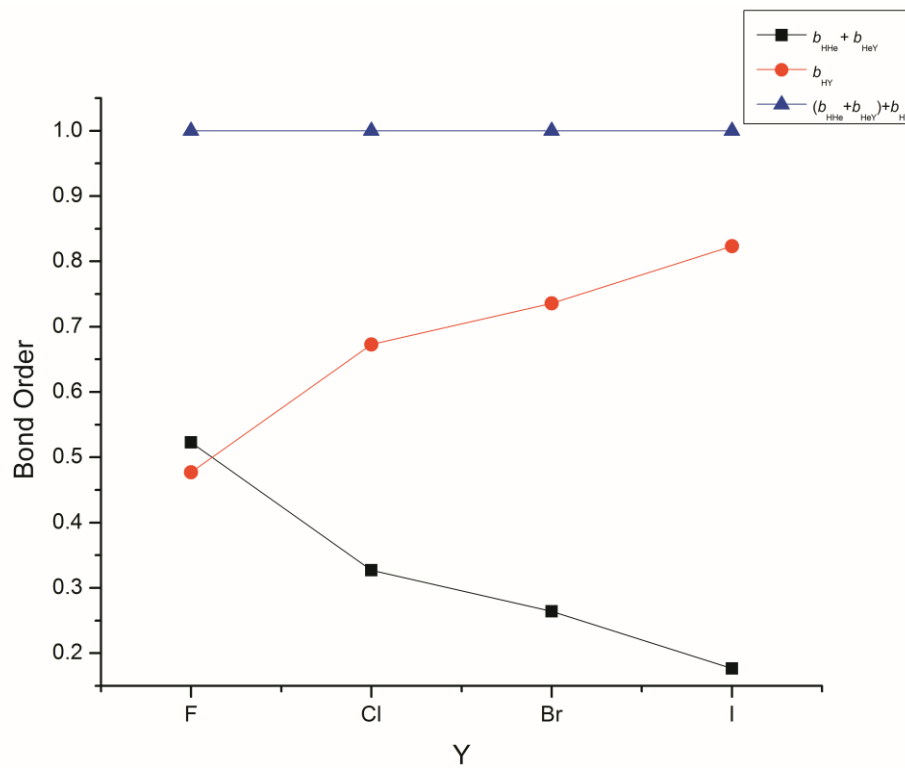


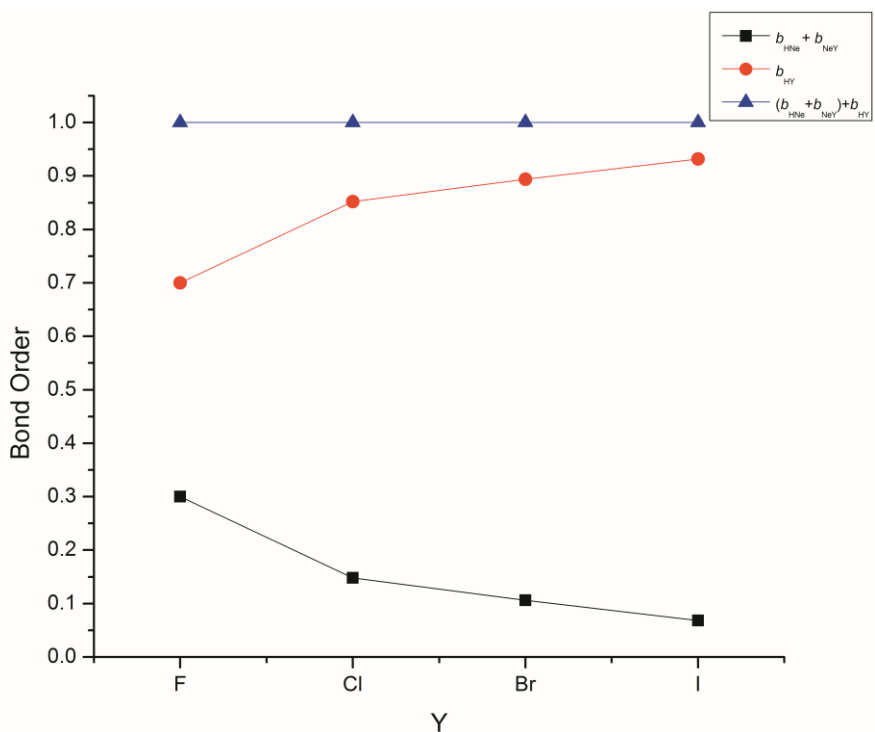
Figure S4. Schematic diagram of competition of 3c/4e ω -bonding and δ -type long-bonding in HHeY (a), HNeY (b), HKrY (c), HXeY (d), HRnY (e), Y=F,

Cl, Br, I.

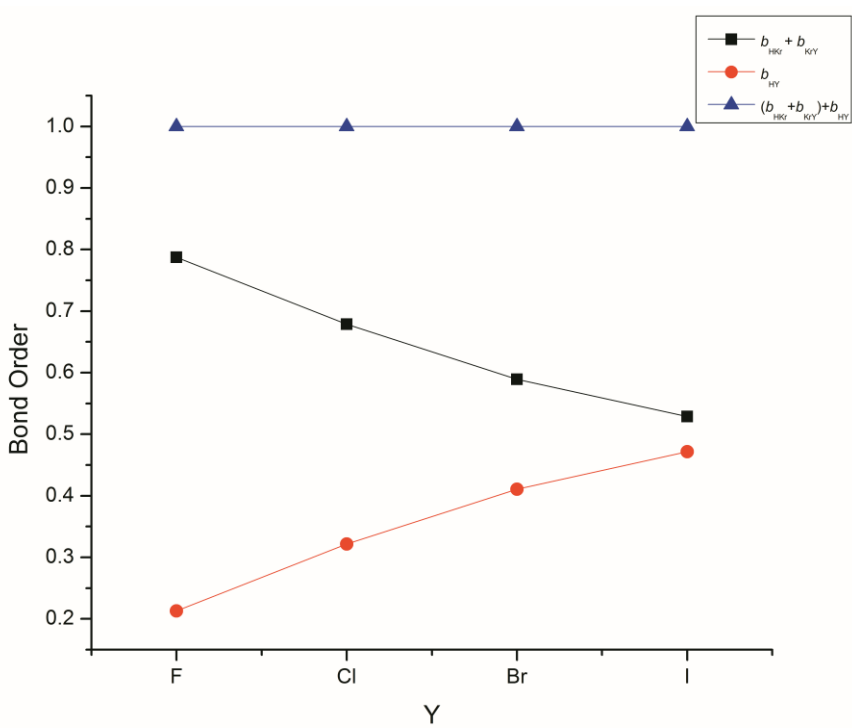
(a)HHeY



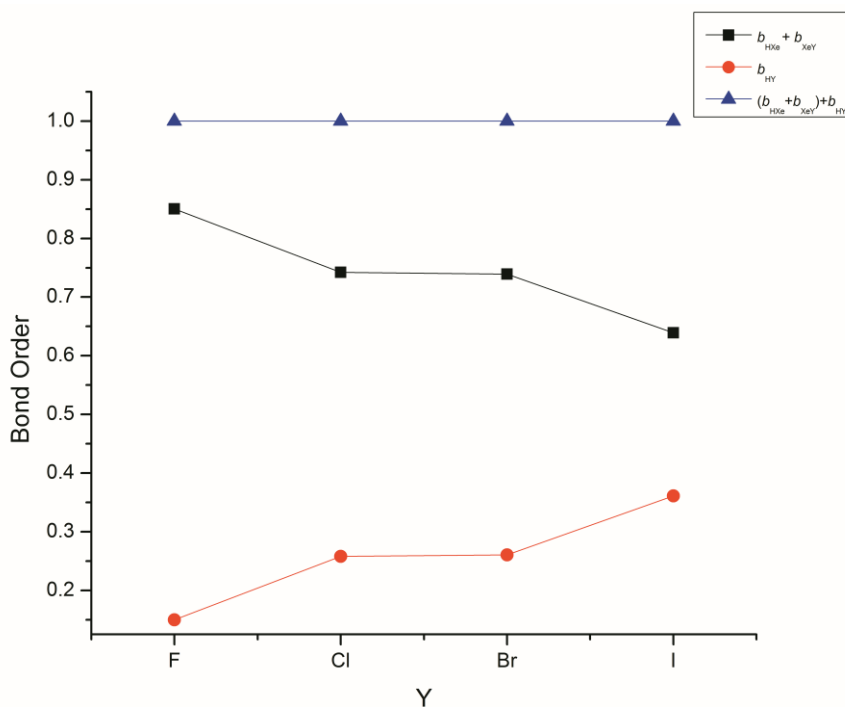
(b)HNeY



(c)HKrY



(d)HXeY



(e)HRnY

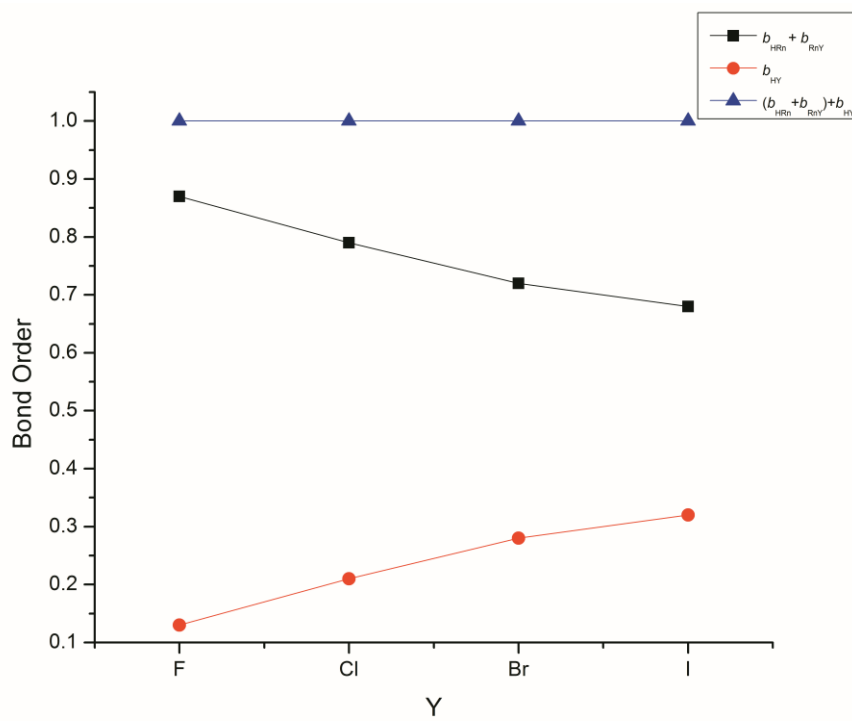
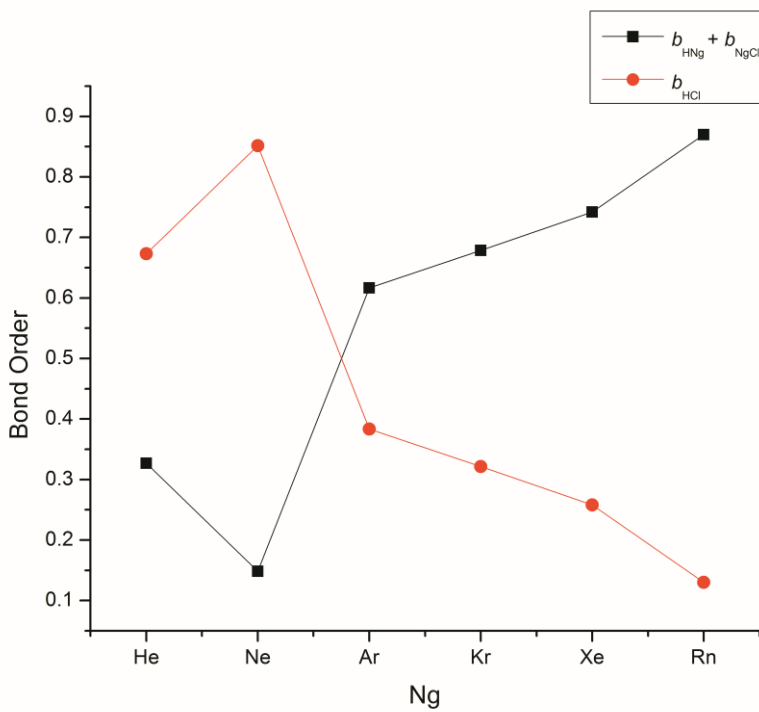
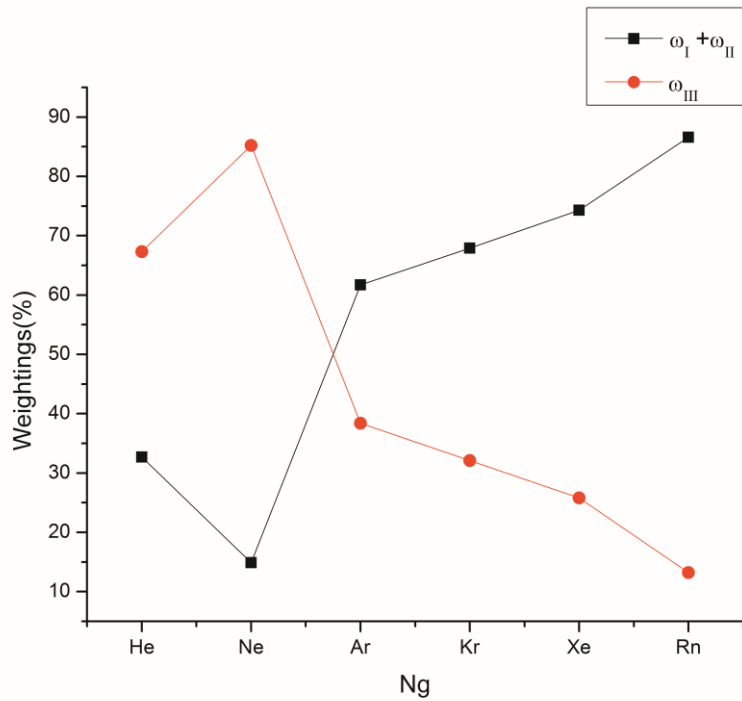
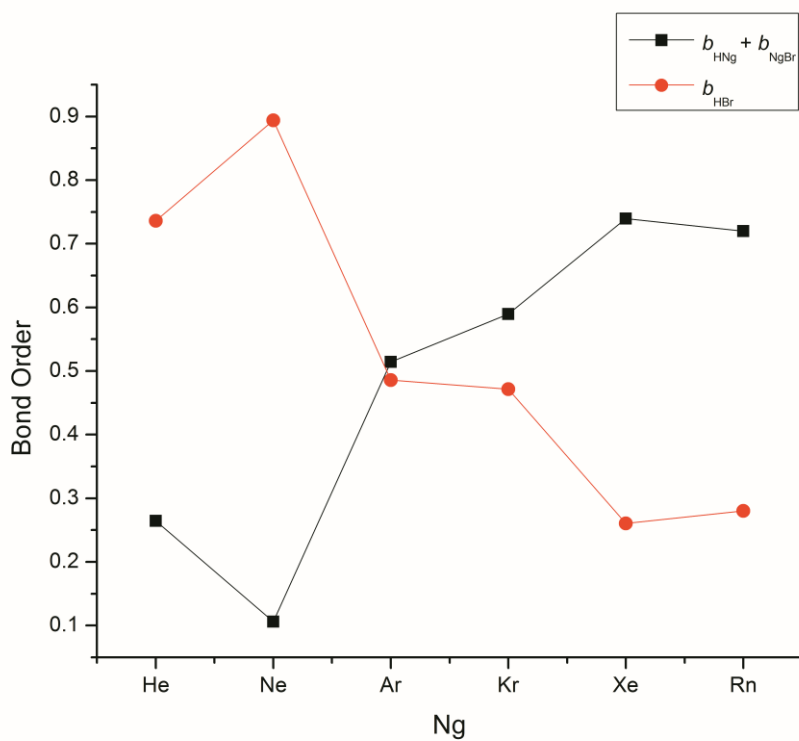
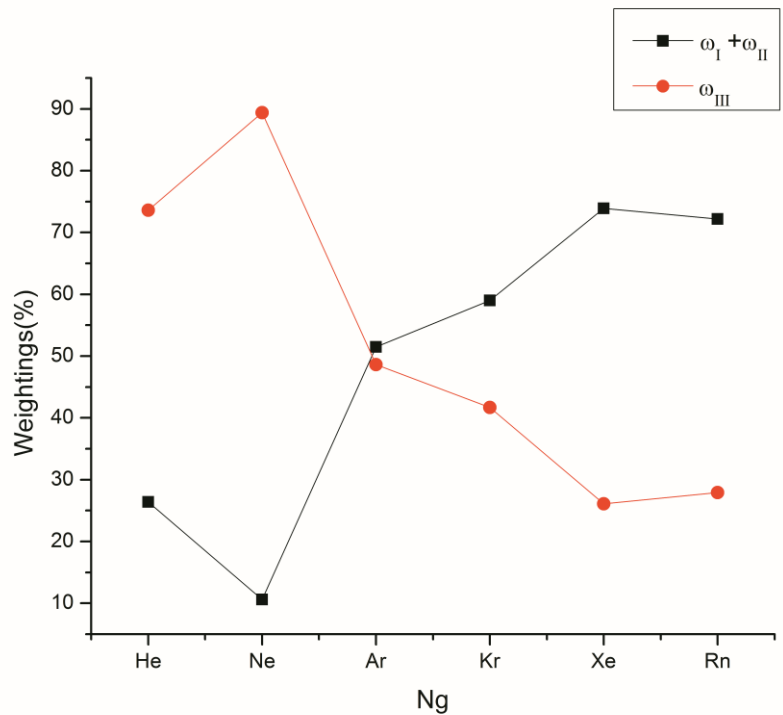


Figure S5. The influence of the central noble-gas atom on the NRT weightings and NRT bond orders of 3c/4e ω -bonded structures and $\hat{\sigma}$ -type long-bonded structure in HNgCl (a), HNgBr (b), HNgI (c), Ng= He, Ne, Ar, Kr, Xe, Rn.

(a)HNgCl



(b) HNgBr



(c) HNgI

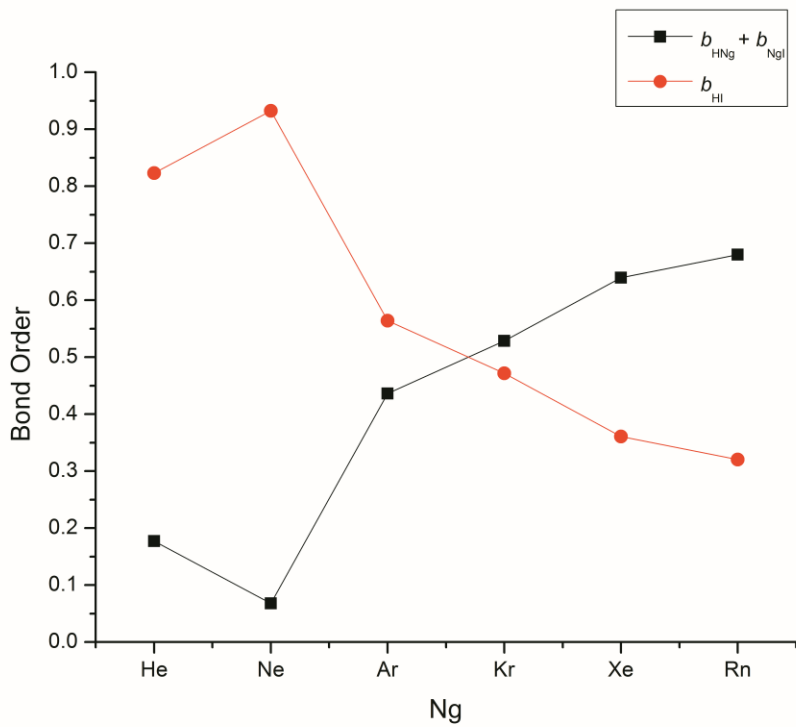
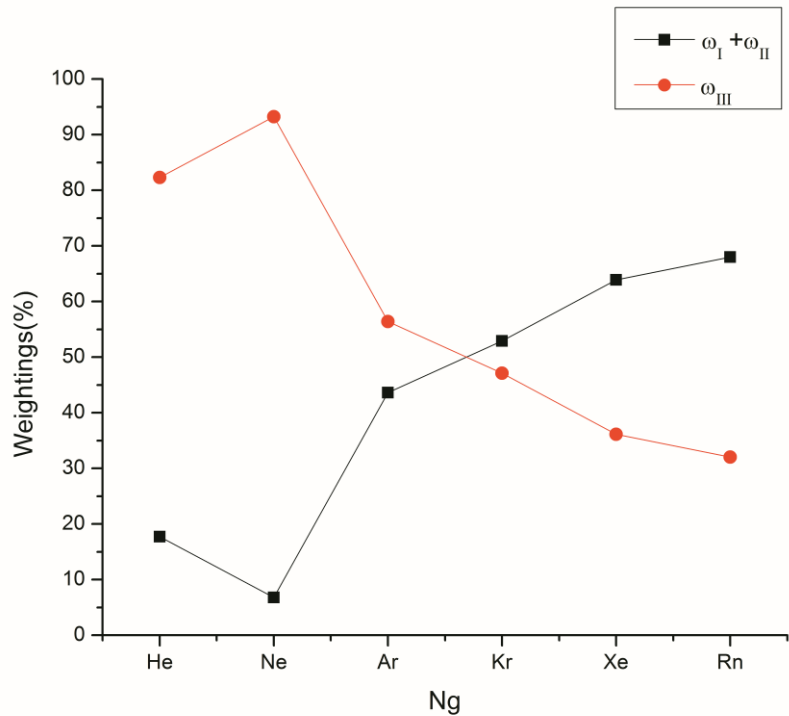
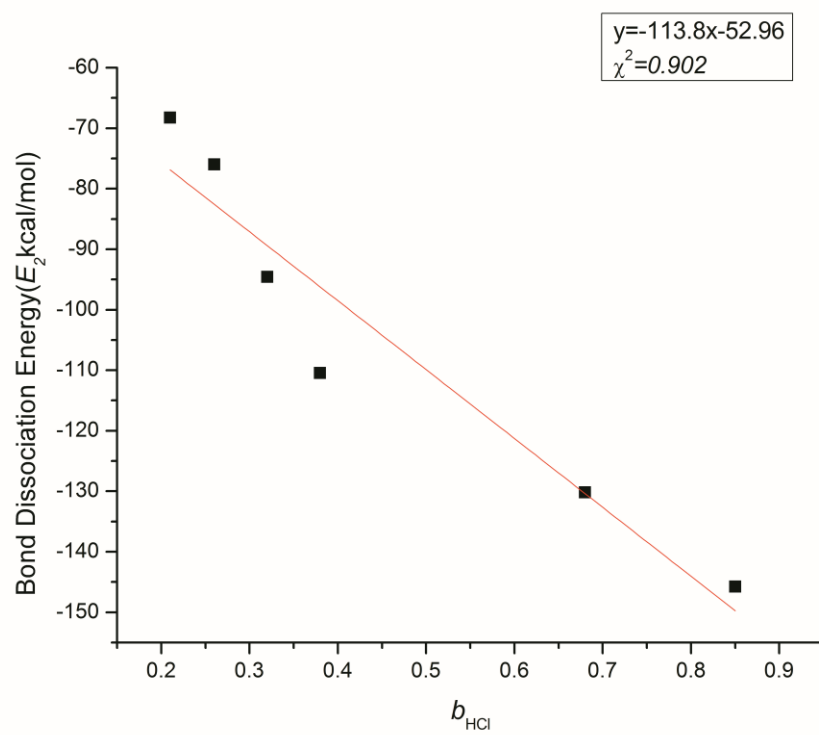
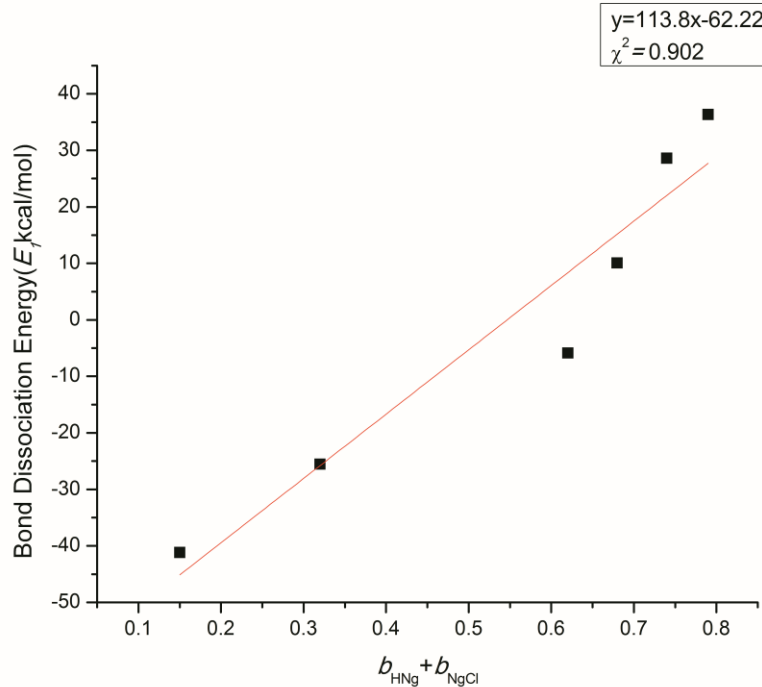
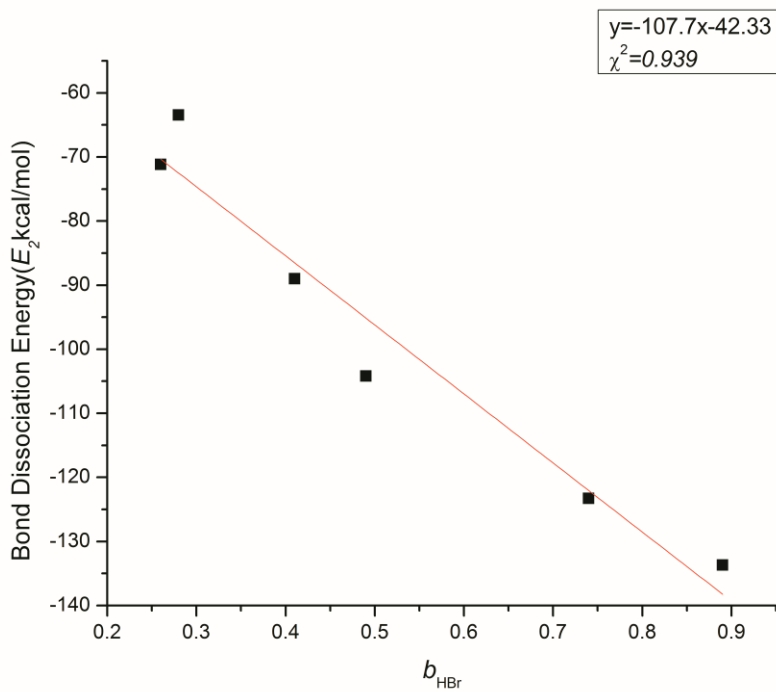
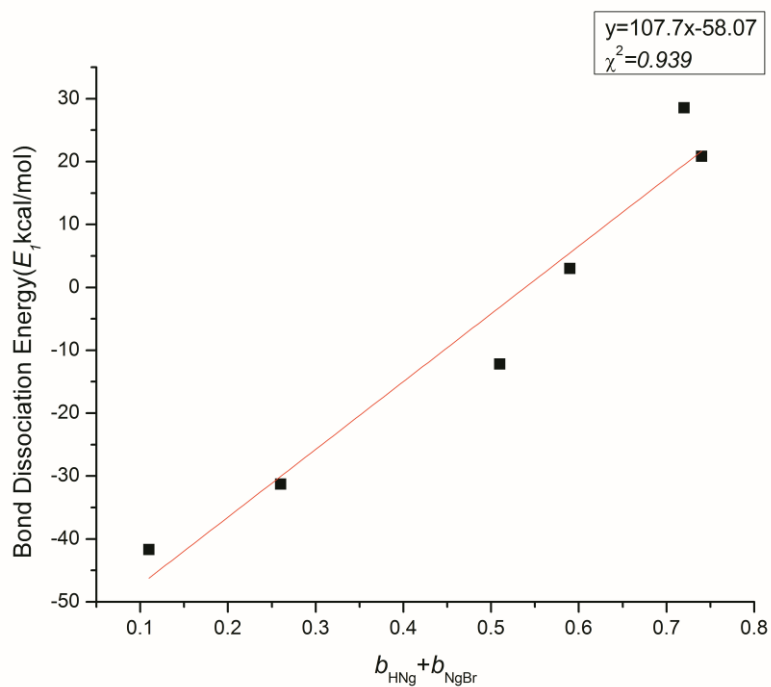


Figure S6. Correlation plots for bond order-bond dissociation energy ($b_{\text{HNg}} + b_{\text{NgY}}$ vs. E_1 and b_{HY} vs. E_2) for HNgCl (a), HNgBr (b), HNgI (c), Ng= He, Ne, Ar, Kr, Xe, Rn.

(a)HNgCl



(b) HNgBr



(c)HN_gI

